

DARK ENERGY AND THERMONUCLEAR SUPERNOVAE

INMA DOMÍNGUEZ

Dpto. de Física Teórica y del Cosmos, Facultad de Ciencias, Universidad de Granada, E-18071 Granada, SPAIN

EDUARDO BRAVO

Dpto. de Física i Enginyeria Nuclear, Universitat Politècnica de Catalunya, Diagonal 647, 08028 Barcelona, SPAIN

LUCIANO PIERSANTI , AMEDEO TORNAMBE , OSCAR STRANIERO

Osservatorio Astronomico di Collurania-INAf, Via Mentore Maggini 47, 64100 Teramo, ITALY

PETER HÖFLICH

Dept. of Physics, Florida State University, 315 Keen Building Tallahassee, FL 32306-4350, USA

Abstract:

Nowadays it is widely accepted that the current Universe is dominated by dark energy and exotic matter, the so called Standard Model of Cosmology or Λ CDM model. All the available data (Thermonuclear Supernovae, Cosmic Microwave Background, Baryon Acoustic Oscillations, Large Scale Structure, etc.) are compatible with a flat Universe made by $\sim 70\%$ of dark energy. Up to now observations agree that dark energy may be the vacuum energy (or cosmological constant) although improvements are needed to constrain further its equation of state. In this context, the cosmic destiny of the Universe is no longer linked to its geometry but to the nature of dark energy; it may be flat and expand forever or collapse. To understand the nature of dark energy is probably the most fundamental problem in physics today; it may open new roads of knowledge and led to unify gravity with the other fundamental interactions in nature. It is expected that astronomical data will continue to provide directions to theorists and experimental physicists. Type Ia supernovae (SNe Ia) have played a fundamental role, showing the acceleration of the expansion rate of the Universe a decade ago, and up to now they are the only astronomical observations that provide a direct evidence of the acceleration. However, in order to determine the source of the dark energy term it is mandatory to improve the precision of supernovae as distance indicators on cosmological scale.

Keywords: Stellar Evolution Models – White Dwarfs – Supernovae – Cosmology.

1 Introduction

Two papers, published a decade ago, marked for the scientific community the beginning of the accelerating Universe: *Observational evidence from supernovae for an accelerating universe and cosmological constant* (September, 1998 [1, 2]) by the High-z Team and *Measurements of Ω and Λ from 42 high-redshifts supernovae* (June 1999 [3]) by the Supernova Cosmology Project. The first one is based on the data of 10 SNe up to $z=0.62$ and the second one on the data of 42 SNe up to $z=0.83$.

These two independent teams got the same result: acceleration of the expansion and, consequently, a nonzero Λ . Note that they were trying to measure the opposite, the deceleration of the expansion, and, moreover, this surprising result was based on the fact that the objects were dimmer than expected; it was unlikely that for any unknown reason less luminous objects were by chance observed instead of the brighter ones.

This exotic component was the missing piece in the Universe component puzzle and finally several long standing problems converged to a solution. *The Cosmological constant is back*, was the title of a paper published by Kraus & Turner in 1995 [4], 3 years before the SNe Ia results came out. Since the beginning, the analysis of Cosmic Microwave Background radiation [5, 6, 7] favoured a flat geometry and other independent set of observations, like the large scale structure of the Universe, favoured a low density-matter Universe, compatible with 30% matter [8]. All three experiments are in perfect agreement and in order to have $\Omega_\lambda=0$, two of them would have to contain severe systematic errors [9].

Additionally, as an accelerating Universe is older (~ 14500 Ma assuming a Hubble constant of 65 km/s/Mpc), the old problem with respect to the age of the oldest globular clusters is *nearly* solved (in our opinion globular cluster would better fix in a *slightly* older Universe).

Evidence for cosmic acceleration has gotten stronger in all these years and nowadays, all efforts focus on characterizing the dark energy equation of state (EOS). The simplest equation relates pressure and density by a parameter, $P = w\rho$; w may be a constant ($w=-1$ for the Cosmological constant or vacuum energy) or vary with redshift. Observations have not provided any evidence that dark energy is not the energy related to the quantum vacuum ($w=-1$ and constant) although theory does not explain it. Empty space is not really empty, particle-antiparticle pairs appear and disappear existing for very brief time but current estimation of the corresponding vacuum energy is 10^{120} times more than needed to explain the acceleration. It is probably the biggest discrepancy between theory and observations in all physics. Matter dilutes as the Universe expands while the vacuum energy remains constant; hence, the matter term dominated in the past while vacuum energy will completely dominate in the future. So, if vacuum energy is really the dark energy, why its density is now so close to that of matter? It is important to understand better the energy of

nothing.

A strong indication in favour of $w = -1$ has come from SNIa Hubble diagrams, which currently includes 200 SNe up to $z = 1.8$; in fact, they show the expected deceleration at $z > 0.5$, and recent acceleration [10].

The future is promising: several experiments, aimed to elucidate the properties of dark energy, are underway or planned from ground based telescopes, from the space, accelerators, and underground laboratories.

Note that the only direct-direct evidence of the acceleration of the expansion rate of the Universe is provided by SNIa Hubble diagrams. It is worth to extend the observations to $z > 1$ where the early effects of deceleration may be detectable [10] and to improve supernova distances and analyze their limits for precision measures of dark energy.

2 Thermonuclear supernova Hubble diagrams: A component with negative pressure is needed

SNIa Hubble diagrams have been used for cosmological applications since 1968 [11]; at that time the dispersion was 0.6 mag. Later on, core-collapse events were identified (Ib) and Hubble diagrams, based only on Type Ia, improved. At the beginning, SNe Ia were considered to be very similar, if not identical, each other, but it became soon evident that this hypothesis was not correct. In 1991, the discovery of the superluminous 1991T and the subluminous 1991bg pointed out that Type Ia were not standard candles.

In 1993 Phillips [12] showed that for a number of near and well observed SNe Ia, whose distance was *a-priori* determined by means of *bona fide* distance indicators, there exists a linear correlation between maximum luminosity and decline rate of luminosity after maximum: peak luminosity decreasing with an increasing decline rate. Basing on this evidence, these Supernovae can be considered once again as an homogeneous class and they can be used as *calibrated candles* using the maximum-decline relation or equivalents [12, 13, 14, 15, 16]. These relations have been improved, mainly by extinction corrections, up to a dispersion of $\sigma \leq 0.18$.

At the same time, the technics to discover high- z SNe developed [17] and *big* CCDs were constructed, like the *Big Throughput Camera* by Tyson and Bernstein that became available for the community at Cerro Tololo and was soon used by the two teams, High- z Team and SN Cosmology Project. An amazing result came out and, since then, our understanding of the Universe completely changed. The conclusion was that SNe Ia located at $0.4 \leq z \leq 0.9$ were about 0.2 magnitudes dimmer than nearby SNe, meaning that they were located further than expected for a constant expansion rate of the Universe (an empty Universe). A negative pressure was required to balance the gravity effects and accelerate the expansion.

Most important, the observations of Type Ia supernovae by themselves indicate the existence of dark energy [18] and show deceleration at $z \geq 0.5$, and acceleration at lower z , ruling out pure acceleration and gray-dust absorption, all at 99% confidence level. Note that these results are obtained with a dispersion in the calibration relation of the order of $\sigma \leq 0.2$ magnitudes.

2.1 EOS of dark energy: A precision better than 0.02 mag is required

Present and future experiments focus on better characterizing the equation of state (EOS) of dark energy. When SNe Ia are used to characterize w , two constraints are usually assumed, a flat ($\Omega_{tot} = 1$) and low-matter density ($\Omega_m = 0.3$) Universe. Notwithstanding these assumptions, it is necessary to have an accuracy of better than 0.02 magnitudes to discriminate between Universes with different w and it is clear that systematic effects will limit our progress.

It is noteworthy that, without the a priori constraint of a flat Universe, the cosmological parameters that best fit Type Ia SNe measurements may be $\Omega_\lambda=1.57$ and $\Omega_m=0.79$ [19].

Now it is mandatory to reduce the current scatter in the calibration relation by a factor of 10, otherwise we may have already reached SNIa limits to measure Cosmology.

3 Systematic effects

The reliability of the maximum-decline relation when it is applied outside the local sample depends on the identification of systematic effects. The high redshift sample could be contaminated with peculiar Ia and with core collapse Ib/c SNe. Some nearby underluminous SNe, like 2002cx [20], 2005hk [21] and 2005bl [22] are well outside the maximum-decline relation although in these cases spectra, taken at the epoch of maximum light, easily reveal their different origin.

However, this approach does not always work; SN2003fg at $z = 0.2$ [23] appears normal at all levels, except for the high luminosity, and it is well outside the maximum-decline relation. In fact, a super-Chandrasehar white dwarf (WD) has been proposed as its progenitor.

Other sources of uncertainty could be K-corrections, the correction that has to be applied to account for the differences caused by the spectrum shifting; the light of the SN is shifted to longer wavelengths while astronomical observations are made in fixed band passes on Earth (e.g., R-band matched to B-band at $z = 0.5$). The error due to uncertainties in this correction is estimated to be small, ~ 0.01 mag [9].

Uncertainties of major concern are those related with potential evolutionary effects: dependence of the SN properties on redshift, changes in the extinction law and, if SN are sensitive to their progenitors, changes in the stellar populations from which they originate.

In the local Universe we see SNe Ia in a variety of environments, some of them with significant extinction and part of them with *peculiar* extinction laws [24]. The properties of the intervening dust may be different going back in time; e.g., a smaller contribution from low mass red giants due to their longer evolutionary times. As the number of SNe Ia increases it is possible to construct Hubble diagrams with subsamples; e.g., only SNe occurring in passive galaxies, less affected by absorption. Most interesting, it has been shown that SNe Ia are good standard candles in the IR; at these wavelengths the extinction is smaller and SNe Hubble diagrams in the IR are promising [25].

4 Observed dependence of SNIa properties on their host galaxies

Great efforts have been devoted in recent years to elucidate the observed dependence of the SN properties on the populations from which they originate. The first studies [26, 27, 14, 28, 29] revealed a dependence of SN properties on their host galaxies: slower light curves (LCs) (brighter SNe) do not occur in ellipticals, while the number of Type Ia SNe, per unit mass, is higher in late type galaxies than in ellipticals [30, 31] and, in star forming galaxies, the SN rate is higher in disks than in bulges [32].

Recently, Mannucci et al. [33] reported that the SNIa rate in late type galaxies is a factor ~ 20 higher than in E/S0. Sullivan et al. [34] focused on the high-redshift sample and qualitatively derived similar trends to those obtained previously for the local Universe: (1) rates are higher (10 times) for strong star-forming galaxies than for galaxies without star formation, (2) slow-decline (bright) SN are only hosted by star-forming galaxies, while non-star-forming galaxies only host fast-decline (dim) SNe and (3) none of the dimmer SNe are found at high-redshift. Except for the most underluminous SNe, the distribution is identical for the high and the low-redshift samples.

These results imply that SNe come from at least two different stellar progenitors, old and young, that differ in 2-3 Gyr, and that their LCs properties are different, depending on those progenitors. At this point, we should note that the empirical calibration used in Cosmology is based on SNe coming from all types of galaxies and thus, the differences due to stellar populations in the nearby Universe are already within the brightness-decline relation. At the other hand, the relative contribution of the two components is expected to evolve strongly with time [35, 34]. A good understanding of the calibration relation in different environments will be essential

to fully exploit SNe Ia in measurements of w .

5 Our understanding of thermonuclear SNe

5.1 What we understand

Type Ia SNe are considered to be the thermonuclear explosion of carbon-oxygen (CO) WDs with a mass close to the Chandrasekhar mass [36]. Starting from such a structure and with a proper explosion mechanism, most of the observed properties are reproduced. The LC is powered by the radioactive energy coming from the decay of ^{56}Ni to ^{56}Co and ^{56}Co to ^{56}Fe and the maximum luminosity depends mainly on the ^{56}Ni mass.

In fact, we have learnt a lot from observations and from one dimensional (1D) numerical simulations. Little carbon is observed in the spectra, indicating that nearly all the WD is burnt, which implies that the explosion (nuclear) energy is similar in all events and excludes a pure deflagration (subsonic burning front) that would leave an observable amount of matter unburnt in the outer part (see [37, 38] and references therein). Final kinetic energies are also similar, as the binding energy, which depends on the total mass and central density of the WD, is not expected to be very different. Intermediate mass elements (e.g. Si, Ca, Mg) are observed in the spectra around maximum light, implying that the external layers have experienced incomplete burning. This excludes a pure detonation (supersonic burning front) that would burn all the WD to Ni and others Fe-peak elements. The delayed detonation models [39, 40], in which the burning front is initially subsonic and at some point accelerates to supersonic velocities, fulfil the observational constraints. In these models, the inner part is completely burnt during the first deflagration phase while the external layers expand, the density decreases, and the right nucleosynthesis, a combination of complete and incomplete burning depending on density, is obtained. Moreover, if the transition from a deflagration to a detonation is delayed (or anticipated), the amount of ^{56}Ni decreases (or increases) and the observed range of luminosities at maximum is reproduced.

Many studies have shown that the delayed detonation explosion of a Chandrasekhar mass (M_{Ch}) WD satisfactorily explains most of the observed properties: the evolution of the LCs and spectra in the optical and in the IR, and also, the observed correlations, including the crucial maximum decline relation [41, 42, 43, 44, 45, 46, 47, 38].

For the reasons above, we have adopted this explosion mechanism and we have kept constant the needed parameters in the description of the deflagration velocity and the critical transition density: the density at which the change from a deflagration to a detonation takes place.

5.2 What we do not understand

The basic ideas explaining SNe Ia as the thermonuclear explosion of a CO WD with a mass close to M_{Ch} were established half a century ago but, in spite of all the dedicated resources, two reasons still prevent our full understanding of these events: (a) the nature and evolutionary history of the progenitor stellar system and (b) the characteristics of the explosion.

Single stellar evolution provides CO WDs with a maximum mass of around $1.1 M_{\odot}$; when a CO core with a higher mass is formed, C is ignited [48]. Binary systems give the possibility of accreting mass from the companion and also explain that this explosions occur in passive galaxies where star formation ended several Gyrs ago. However, how a typical WD of 0.6 to $1 M_{\odot}$ could reach the Chandrasekhar mass by accretion is still a matter of hot debate. Accretion of H or He from a non-degenerate companion is referred as the Single Degenerate (SD) scenario while accretion of C and O, from a thick disk formed from the merging of two WDs, is referred as the Double Degenerate (DD) scenario.

In the first case the donor is a normal star with an Hydrogen rich envelope [49]. These systems are well studied and they are associated with a variety of observational events (symbiotic stars, classical novae, cataclysmic variables, dwarf novae, recurrent novae and many others). However, in our opinion this scenario is not promising as SNe Ia progenitor since during the accretion process some instabilities arise, thus preventing the growth in mass of the CO core up to the Chandrasekhar limit [51]. For a different view see [50] and references therein.

The second scenario envisions a system composed by two tidally interacting WDs with total mass of the order of or greater than the M_{Ch} . In this case the two stars, due to gravitational wave radiation (GWR) emission, undergo a merging so that the less massive component completely disrupts, thus forming an accretion disk around the more massive one [53, 54]. In this case C-O rich matter is directly accreted. One major concern afflicts the DD scenario: the accretion rate which results after the merging would be so high that off-center carbon ignition occurs well before the WD could attain the limiting mass, thus producing as final outcome not a SNe Ia event, but an O-Ne white dwarf which eventually collapses into a neutron star [55, 56, 57]. The historical concern about the existence or not of observed counterparts of these systems seems to have been solved in favor of their existence [58]. Later on, we will show that, when the rotational effects are taken into account in modeling the binary system, the evolution from the merging of the two CO WDs up to the final explosive outcome is not only possible, but it results mandatory. Moreover, recent studies of observational properties of known Type Ia supernova remnants in the Galaxy favour the DD scenario [59].

Concerning the explosive phase, once C is ignited, the burning conditions are not reached by the compression of subsequent shells by the pressure wave (detonation). If

so, all the WD would be transformed to Fe-peak elements and no intermediate mass elements would be produced. On the other hand, if subsequent zones are heated only via thermal conduction, the velocity of the flame would be too low and the pressure wave would expand the WD till low densities, quenching the flame. However, turbulent mixing of the unburnt cold matter with the hot ashes is expected to occur and instabilities, like the Rayleigh-Taylor instability, develop. In this case the velocity of the burning front will be determined by the growth rate of these instabilities, being still subsonic but reaching soon values higher than those corresponding to the conductive velocity.

In 1D models, we rely on parametrization of this 3D turbulent mixing. The simple way is to assume a flame velocity equal to a few percent of the sound velocity [60]. The flame travels outward through lower and lower densities and would quench before reaching the surface. As quoted above, the observations require that all the WD is burnt; therefore, at some point, the flame velocity has to be increased as it happens in the delayed detonation models quoted before [39]. However, the physics of the transition to a detonation in unconfined environments, like in current Type Ia SN models, is not completely understood [61]. This transition is expected to depend on the properties of the structure, like the chemical gradient of fuel (*Zeldovich induction mechanism*) and, hence, on the progenitor.

Current 3D simulations are still far from a complete and successful explosion and even farther from being able to follow simultaneously all the relevant scales [62, 63, 64, 65, 66, 67]. As a consequence, successful explosions are still 1D simulations, being the assumed transition density (or the equivalent pre-expansion time) the main factor determining the amount of ^{56}Ni produced and therefore, the maximum luminosity and LC shape.

5.3 Any observed hints from the companion?

A great observational effort is being done to identify the elusive companion of the exploding WD. First detections have been reported, although a clear answer has not yet been achieved. The spectra of 2002ic [68] show interaction with the circumstellar medium, hydrogen is abundant and an AGB star was identified as the companion. However both of the proposed scenarios (SD and DD) could explain this event [69] and, recently, it has been proposed that it was a core-collapse SN instead of a SNIa [70].

Interaction with the circumstellar medium is also detected in the case of 2006X [71] and a red giant has been proposed as the companion, favouring the SD scenario. However, note that H-lines are not seen in the spectra.

Another possibility is to look for the companion in nearby Type Ia SN-remnants, this has been done for the Tycho's supernova (SN 1572); Ruiz-Lapuente [72] claimed the identification of the donor star, Ihara [73] argue that this is not a viable object.

Finally, a very interesting case is the recurrent nova RS-Oph, for which the mass of the accreting WD is estimated to be very close to M_{Ch} , $\sim 1.38 M_{\odot}$, and it is still increasing [74, 75]. Note that in this case there is H present in the system and in fact H is observed.

6 Influence of the progenitor of the exploding WD on SNIa properties

Let us now address the question of the influence of the WD progenitor on the final outcome. First, we will analyze the dependence of the final chemical composition of the WD on the initial mass of its progenitor, and then we will study how the light curves properties depend on this composition. Then, we will repeat the same analysis but considering the dependence of the WD progenitor properties on the metallicity. Note that given the *standard* model, a Chandrasekhar-mass CO WD, not much space is left for variations. In this set of models, the differences among the WDs are due to chemical composition differences: carbon and oxygen abundances and chemical gradients. This translates into differences in the ^{56}Ni mass synthesized during the explosion and therefore, differences in the LCs.

We have considered the entire range of potential progenitors, with main sequence masses from 1.5 to $7 M_{\odot}$ and metallicities between $Z = 0$ and 0.02. The pre-supernova evolution, starting from the pre-main sequence phase, is simulated by means of a 1D hydrostatic code, the FRANEC code [76, 77, 78, 79]. Starting from the computed WD structures, we simulate the explosion, including detailed nucleosynthesis, and obtain the LCs [43, 80]. The single degenerate scenario has been assumed; the WD reaches the M_{Ch} by accretion of H from a non-degenerate companion.

6.1 Influence of the Initial Mass

We identify the initial mass of the progenitor (main sequence mass) of the exploding WD as a key parameter in the evolution; it modifies the average C/O ratio in the WD by up to 22% and thus, the kinetic energies and ^{56}Ni masses [80].

We could distinguish two regions in the exploding structure: the inner one, the original WD (with masses between 0.55 and $0.99 M_{\odot}$, corresponding to initial masses between 1.5 and $7 M_{\odot}$) and the external one, formed by the accreted matter. The C/O rate is determined by the previous He-burning phases. Initially carbon is produced via the 3α reactions and once sufficient ^{12}C is synthesized, the $^{12}\text{C}(\alpha, \gamma)^{16}\text{O}$ reaction becomes competitive with the 3α , and carbon is partially burned into oxygen. The amount of C/O is greater (~ 1) in the accreted matter because in these layers the $^{12}\text{C}(\alpha, \gamma)^{16}\text{O}$ reaction does not have enough time to destroy ^{12}C (unlike the situation during central convective He-burning). This higher C/O rate in the

previously accreted layers is critical for the final average C/O within the exploding structure.

The results are summarized in Table 1, where we report from column 1 to 6: (1) initial Z and Y, (2) initial (main sequence) mass, (3) mass of the CO core at the beginning of the thermal pulse phase, (4) C abundance (mass fraction) at the center, (5) averaged C/O rate within the final $\sim 1.37 M_{\odot}$ CO white dwarf after accretion, and (6) ^{56}Ni mass synthesized during the explosion.

More massive progenitors accrete less mass, as a consequence the final average C/O is smaller, less ^{56}Ni is synthesized, the SNIa is less luminous, the LC-decline is faster and expansion velocities are smaller (up to 2000 km/s considering the whole range). Notice that the correlation between LC shape and expansion velocity could be used to further reduce the scatter in the calibration relation. The size of this effect on the maximum magnitude, $\Delta M_{max} \sim 0.2$ mag, is critical for the reconstruction of the cosmological equation of state.

In Figure 1 the final C and O profiles (mass fraction) are shown for some selected models with different initial (main sequence) mass and Z.

	$M_{MS}(M_{\odot})$	$M_{CO}^{TP}(M_{\odot})$	C_{cen}	C/O_{Mch}	$^{56}\text{Ni} (M_{\odot})$
Z=0.02	1.5	0.55	0.21	0.75	0.589
Y=0.28	3.0	0.57	0.21	0.76	0.584
	5.0	0.87	0.29	0.72	0.561
	7.0	0.99	0.28	0.60	0.516
Z=10 ⁻³	1.5	0.59	0.24	0.76	0.587
Y=0.23	3.0	0.77	0.26	0.74	0.567
Y=0.23	5.0	0.90	0.29	0.66	0.541
	6.0	0.98	0.29	0.60	0.522
Z=10 ⁻¹⁰	5.0	0.89	0.32	0.70	0.549
Y=0.23	7.0	0.99	0.31	0.62	0.525

Table 1: Properties of the models.

6.2 Influence of the initial metallicity

As it is shown in Table 1, the mass of the CO core does not depend markedly on the initial metallicity of the progenitor; the only exception being the $3 M_{\odot}$ that at Z=0.02 behaves as a low-mass star. As a consequence, the final chemical composition of the exploding WD is not sensitive to the initial Z [80]. For this reason, the ^{56}Ni mass and the maximum luminosity depend mildly on the initial metallicity.

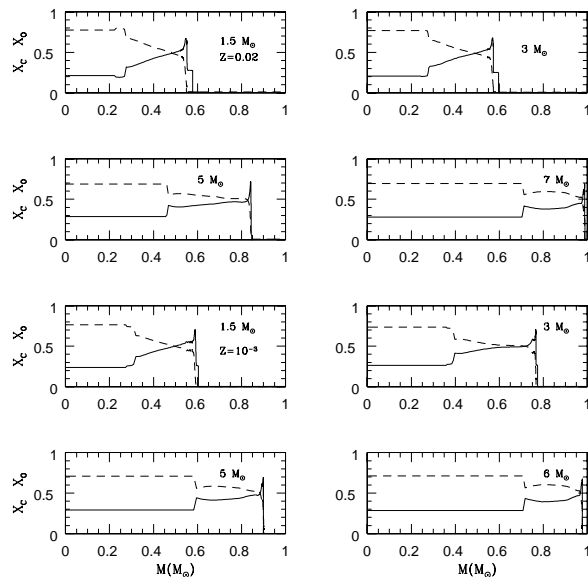


Figure 1: Final chemical Carbon (solid) and Oxygen (dotted) profiles in the central region of stars with initial (main sequence) masses between 1.5 and $7 M_{\odot}$ and for $Z = 0.02$ (upper pannels) and $Z=0.001$ (lower pannels) (see Table 1).

However, the metallicity alters the isotopic composition of the outer layers of the ejecta and few Fe-lines contribute to the opacity. This effect is important at short wavelengths, changing the intrinsic colour index B-V by up to -0.06 mag; moreover, it alters the fluxes in the U band and the UV [81]. The change in B-V is critical if extinction corrections are applied; the metallicity effect can systematically alter the estimates for the absolute brightness by up to 0.2 mag [80].

7 WD rotation and the properties at explosive C-ignition

In this case, we have assumed that two WDs (DD scenario) rotate at the orbital frequency due to the combined action of shear friction and tidal forces. Note that, once synchronization is attained, it will be maintained up to the merging epoch. The heating produced by the frictional stresses determines that two WDs heat up and

become more luminous during the GWR-driven shrinking [83]. Then, the two WDs merge so that the less massive component (the more expanded) completely disrupts, forming a thick disk from which matter flows to the companion. The real initial value of the accretion rate must be close to the Eddington limit. Fortunately, as we have shown, the initial value of this accretion rate does not affect the further evolution at all [82].

On the accreting WD, thermal energy is stored in the external layers while angular momentum is stored in the entire structure, which spins up. Due to the combined effect of these two processes, the accreting structure rapidly expands and accretion comes to a halt due to the onset of the Roche instability. Hence, the heat excess localized into the external layers is removed via thermal diffusion toward the inner zones. As a consequence the structure contracts and spins up. However, due to the redistribution of angular momentum, the angular velocity increases more slowly than the critical velocity and accretion is restored. It is as if there exists a gate which can be closed or open, depending on the actual physical conditions of the accreting WD. If such a process continued indefinitely, with no additional physics coming into play, the mean accretion rate would decrease with time and the self-tuned accretion mechanism would come to a definitive halt well before the Chandrasekhar mass is attained. However angular momentum is expected to be lost by gravitational wave radiation and the accretion process continues to occur in a self-regulated fashion until the Chandrasekhar mass limit for non-rotating structures has been already achieved or by-passed [82].

M_{tot} (M_{\odot})	ρ_{ig} (g/cm^3)	ω_{rot} (rad/s)	U_{bin} (foe) ¹	M_{eje} (M_{\odot})	E_k (foe) ²	^{56}Ni (M_{\odot})	M_{bol}
STD							
1.39	$2.90 \cdot 10^9$	0.0	-0.52	1.39	1.09	0.772	-19.48
$\tau_{bra}=10^4$ yr							
1.39	$2.17 \cdot 10^9$	1.07	-0.53	1.39	1.15	0.819	-19.58
1.42	$2.08 \cdot 10^9$	1.80	-0.56	1.42	1.17	0.847	-19.61
1.45	$2.09 \cdot 10^9$	2.27	-0.59	1.45	1.17	0.857	-19.61
1.48	$3.34 \cdot 10^9$	3.08	-0.66	1.30	1.04	0.817	-19.52
$\tau_{bra}=10^5$ yr							
1.39	$3.14 \cdot 10^9$	0.78	-0.53	1.36	1.08	0.774	-19.50
1.42	$2.84 \cdot 10^9$	1.92	-0.57	1.42	1.11	0.813	-19.56
1.45	$2.75 \cdot 10^9$	2.49	-0.61	1.44	1.12	0.837	-19.59
1.48	$3.01 \cdot 10^9$	3.02	-0.66	1.37	1.07	0.835	-19.55

¹ 1 foe= 10^{51} erg

Table 2: Properties of the rotating models.

Models with WD masses ranging between 1.4 and 1.5 M_{\odot} have been analyzed. Differentially rotating WDs may be stable up to several solar masses but here rigid body rotation has been assumed so that the corresponding Chandrasekhar limit is $\sim 1.5 M_{\odot}$. As in the previous section, we assume the delayed detonation explosion mechanism, keeping constant the transition density for all our experiments, and compute the explosions and light curves [84, 85, 86]. This is the only reasonable choice to disentangle the effects of rotation on the observational properties of explosive events.

To slow down the WD a braking efficiency is assumed, physically motivated by the frictional viscosity due to the interaction of the WD with the accretion disk [82].

Our main results are summarized in Table 2: (1) total mass, (2) ignition density, (3) angular velocity at ignition-time, (4) total binding energy, (5) ejected mass, (6) kinetic energy (7) mass of ^{56}Ni produced in the explosion and (8) bolometric magnitude at maximum time. Model *STD* is a reference model, without rotation, while τ_{bra} refers to the adopted values for the time scale describing the braking efficiency.

At the time of explosive carbon ignition, the ignition density varies by 46%; the higher values, $\sim 3 \cdot 10^9 \text{ g/cm}^3$, are reached in the more massive models. This trend is also shown by the binding energies (with a variation of about 22%).

The amount of ^{56}Ni produced depends on the binding energy and on the ignition density, and the two factors act in opposite directions. More massive models have greater binding energies and greater ignition densities; more energy has to be invested to unbind the WD, implying less final kinetic energy and a larger completely incinerated zone. However, electron captures are also favoured in the inner high density region, so that the production of ^{56}Ni does not show a monotonic dependence with the ignition density, binding energy or total mass. The spread in ^{56}Ni mass ($\sim 0.08 M_{\odot}$) translates into a difference at maximum of 0.11 mag (see Figure 2).

8 Summary and conclusions

SNIa Hubble diagrams show the existence of dark energy and how the expansion rate of the Universe changes from deceleration to acceleration at $z \sim 0.5$ [10]. SNIa absolute maximum magnitudes are obtained through a calibration relation that links them with the LC shape, the scatter in this relation is ≤ 0.2 mag.

- Observations have shown that the properties of the LCs and the rate of SNe Ia are related with the properties of their host galaxies; most luminous SNe Ia only happen in galaxies with ongoing star formation, in which their rate is also higher [35, 34]. This may indicate different stellar progenitors for Type Ia with evolutionary times that differ by 2-3 Gyr.
- Our theoretical studies have focused on the dependence of the SNIa properties on their progenitors. We have computed 1D numerical simulations, including

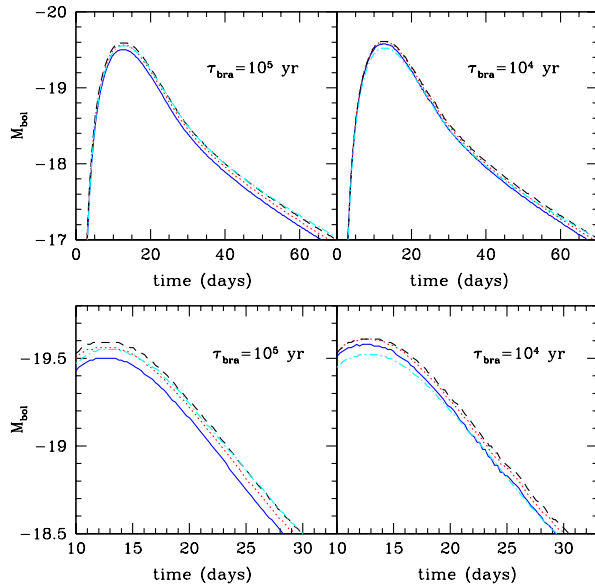


Figure 2: Bolometric light curves for the two set of models showed in Table 2. The spread in ^{56}Ni mass translates into a difference at maximum of 0.11 mag.

stellar evolution, accretion onto the WD, explosions -assuming the delayed detonation mechanism-, detailed nucleosynthesis and light curves. We vary mass and chemical composition of the progenitor of the WD and, in the framework of the DD scenario, total mass of the system and rotational velocity. All these numerical experiments, in which explosion parameters (the crucial transition density) have been kept constant, led to variations at maximum ≤ 0.2 mag [80, 87].

- To characterize the EOS of dark energy using SNe Ia Hubble diagrams, the dispersion on the calibration relation should be reduced by a factor of 10. Otherwise we may have reached the precision limit of SNIa as distance indicators.

SNe Ia are the only astronomical observations that provide a direct evidence of the acceleration/deceleration of the Universe. It is worth to identify SNIa progenitors and explosion mechanism, to improve supernova cosmic distances and to analyze their reliability as precise probe of the dark energy nature.

Acknowledgements: I.D. warmly thanks Minia Manteiga and Ana Ulla for their enthusiasm and for their kind invitation to write this review. This work has been partially supported by the MCyT grant AYA2005-08013-C03-03, by the Spanish-Italian cooperation INFN-CICYT and by the Aspen Center for Physics (2007).

References

- [1] Riess, A. et al. 1998, AJ 116, 1009
- [2] Schmidt B.P et al. 1998, ApJ 507, 460
- [3] Perlmutter et al. 1999, ApJ 517, 565
- [4] Krauss, L.M., Turner, M.S. 1995, General Relativity and Gravitation, 27, 1137
- [5] de Bernardis, P. et al. 2000 Nature 404, 955
- [6] Spergel, D.N. et al. 2003, ApJS 148, 175
- [7] Spergel, D.N. et al. 2007, ApJS 170, 377
- [8] Verde, L., Haiman, Z., Spergel, D.N. 2003, ApJ 581, 5
- [9] Schmidt B.P. 2005, ASP Conference Series, 342
- [10] Riess, A. et al. 2007, ApJ 659, 98
- [11] Kowal, C.T. 1968, AJ 73, 1021
- [12] Phillips, M.M. 1993, ApJL 413, L105
- [13] Phillips, M.M., Lira, P., Suntzeff, N.B., Schommer, R.A., Hamuy, M., Maza, J. 1999, AJ 118, 1766
- [14] Hamuy, M. et al. 1996, AJ 112, 2391
- [15] Perlmutter et al. 1997, ApJ 483, 565
- [16] Riess, A.G., Press, W.H., Kirshner, R.P. 1996, ApJ 473, 88
- [17] Norgaad-Nielson, H.U. et al. 1989, Nature 339, 523
- [18] Knop, R.A. et al. 2003, ApJ, 598, 102
- [19] Clocchiatti, A. et al. 2006, ApJ, 642, 1
- [20] Li, W. et al. 2003, PASP 115, 453L
- [21] Chornock, R. 2006 PASP 118, 722
- [22] Taubenberger, S. et al. 2008, MNRAS, in press (arXiv:0711.4548)
- [23] Howell, D. 2006, Nature 308, 283
- [24] Elias-Rosa, N. et al. 2006, MNRAS 369, 1880
- [25] Krisciunas, K. et al. 2004, AJ 128, 3034
- [26] Branch, D., Romanishin, W., Baron, E. 1996, ApJ 465, 73
- [27] Hamuy, M. et al. 1995, AJ 109, 1
- [28] Hamuy, M. et al. 2000, AJ 120, 1479
- [29] Ivanov, V.D., Hamuy, M., Pinto, P.A. 2000, ApJ 542, 588
- [30] Cappellaro E. et al. 1997, A&A 322, 421
- [31] Cappellaro E. 2003, *Supernovae and Gamma-Ray Burst*, Lec. Notes in Physics 598, 37
- [32] Wang, L., Hoefflich, P., Wheeler, J.C. 1997, ApJL 483, L29
- [33] Mannucci, F. et al. 2005, A&A 433, 807

- [34] Sullivan, M. et al. 2006, ApJ 648, 868
- [35] Mannucci, F., Della Valle, M., & Panagia, N. 2006, MNRAS 370, 773
- [36] Hoyle, W.A. Fowler 1960, ApJ 132, 565
- [37] Marion, G.H. et al. 2006, ApJ 645, 1392
- [38] Mazzali, P., Röpke, F.K., Benetti, S., Hillebrandt, W. 2007, Science 315, 825
- [39] Khokhlov, A. 1991, ApJ 245, 114
- [40] Khokhlov, A. 1995, ApJ 457, 695
- [41] Fisher, A., Branch, D., Höflich, P., Khokhlov, A. 1995, ApJL 447, 73
- [42] Höflich, P. 1995, ApJ 443, 89
- [43] Höflich, P., Khokhlov, A. 1996, ApJ 457, 500
- [44] Wheeler, J.C., Höflich, P., Harkness, R.P., Spyromilio, J. 1998, ApJ 496, 908
- [45] Lentz, E.J., Baron, E., Branch, D., Hauschildt, P.H., Nugent, P.E. 2000, ApJ 530, 966
- [46] Höflich, P., Gerardy, C., Fesen, R.A., Sakai, S. 2002, ApJ 568, 791
- [47] Höflich, P., Gerardy, C., Linder, E., et al. 2003, Lecture Notes in Physics (review), 635, 203
- [48] Becker S. A., Iben I. Jr. 1980, ApJ 237, 111B
- [49] Whelan, J., & Iben, I. Jr. 1973, ApJ 186, 1007
- [50] Hachisu. I. et al. 2007, ApJ 663, 1269
- [51] Piersanti, L., Cassisi, S., Iben, I.Jr., Tornambe, A. 2000, ApJ 535, 932
- [52] Piersanti, L., Gagliardi, S., Iben, I.Jr., Tornambe, A. 2003, ApJ 583, 885
- [53] Iben, I.Jr., Tutukov, A.V. 1984, ApJSS 54, 335
- [54] Webbink, R.F. 1984, ApJ 277, 355
- [55] Nomoto, K.I., & Iben, I.Jr. 1985, ApJ 297, 531
- [56] Saio, H., Nomoto, K. 1985, A&A 150, 215
- [57] Saio, H., & Nomoto, K.I. 1998, ApJ 500, 388
- [58] Napiwotzki, R. et al. 2005, ASPC 334, 375
- [59] Badenes, C., Hughes, J.P., Bravo, E., Langer, N. 2007, ApJ 662, 472
- [60] Domínguez, I., Höflich, P. 2000, ApJ 528, 854
- [61] Khokhlov, A.M., Oran, E.S., Wheeler, J.C. 1997, ApJ 478, 678
- [62] Gamezo, V.N., Khokhlov, A.M., Oran, E.S., Chtchelkanova, A.Y. Rosenberg, R. 2003, Science 299, 77
- [63] Gamezo, V.N., Khokhlov, A.M., Oran, E.S. 2005, ApJ 623, 337
- [64] Plewa, T., Calder, A.C., Lamb, D. 2004, ApJL 612 L37
- [65] García-Senz, D., Bravo, E. 2005, A&A 430, 585
- [66] Röpke, F. K., Hillebrandt, W. 2005, A&A 431, 635
- [67] Plewa, T. 2007, ApJL 657 942
- [68] Hamuy, M. et al. 2003, Nature 424, 651
- [69] Livio, M., Riess, A. G. 2003, ApJL 594, 93
- [70] Benetti, S., et al 2006, ApJ 653, L129
- [71] Patat, F. et al. 2007, Science 317, 924
- [72] Ruiz-Lapuente et al. 2004, Nature 431, 1069
- [73] Ihara, Y. et al. 2007, PASJ 59, 811

- [74] Hachisu, I. et al. 2006, ApJ 615, 141
- [75] Sokoloski, J.L., Luna, G.J.M., Mukai, K., Kenyon, S.J. 2006, Nature 442, 276
- [76] Chieffi, A., Limongi, M., Straniero, O. 1998 ApJ 502, 737
- [77] Domínguez, I., Chieffi, A., Limongi, M., Straniero, O. 1999, ApJ 524, 226
- [78] Straniero, O., Chieffi, A., Limongi, M. 1997, ApJ 490, 425
- [79] Chieffi, A., Domínguez, I., Limongi, M., Straniero, O. 2001, ApJ 554, 1159
- [80] Domínguez, I., Höflich, P., Straniero, O. 2001, ApJ 557, 279
- [81] Höflich, P., Wheeler, J.C., Thielemann, F.K. 1998, ApJ 495, 617
- [82] Piersanti, L., Gagliardi, S., Iben, I.Jr., Tornambe, A. 2003, ApJ 598, 1229
- [83] Iben, I.Jr., Tutukov, A.V., Fedorova, A. V. 1998, ApJ 503, 344
- [84] Bravo, E., Domínguez, I., Isern, J., Canal, R., Höflich, P., Labay, J. 1993, A&A 269, 187
- [85] Bravo, E., A. Tornambe, A., I. Domínguez, Isern, J. 1996, A&A 306, 811
- [86] Badenes, C., Bravo, E., Borkowski, K.J., Domínguez, I. 2003, ApJ 593, 358
- [87] Domínguez, I., Piersanti, L., Bravo, E., Tornambe, A., Straniero, O. Gagliardi, S. 2006, ApJ 644, 21

